

Chemical Properties of Oxidized Silicon Carbide Surfaces upon Etching in Hydrofluoric Acid

Sarit Dhar,^{†,‡} Oliver Seitz,[§] Mathew D. Halls,^{§,||} Sungho Choi,^{†,±} Yves J. Chabal,^{*,§,#} and Leonard C. Feldman^{†,#}

Department of Physics and Astronomy, Vanderbilt University, Nashville, Tennessee, Department of Materials Science and Engineering, University of Texas at Dallas, Richardson, Texas, Materials Science Division, Accelrys, Incorporated, San Diego, California, Institute for Advanced Materials, Devices and Nanotechnology, Rutgers University, Piscataway, New Jersey, and Device Materials Research Center, Korea Research Institute of Chemical Technology, Republic of Korea

Received June 29, 2009; E-mail: chabal@utdallas.edu

Abstract: Hydrogen termination of oxidized silicon in hydrofluoric acid results from an etching process that is now well understood and accepted. This surface has become a standard for studies of surface science and an important component in silicon device processing for microelectronics, energy, and sensor applications. The present work shows that HF etching of oxidized silicon carbide (SiC) leads to a very different surface termination, whether the surface is carbon or silicon terminated. Specifically, the silicon carbide surfaces are hydrophilic with hydroxyl termination, resulting from the inability of HF to remove the last oxygen layer at the oxide/SiC interface. The final surface chemistry and stability critically depend on the crystal face and surface stoichiometry. These surface properties affect the ability to chemically functionalize the surface and therefore impact how SiC can be used for biomedical applications.

I. Introduction

Silicon dioxide (SiO₂) is the single most versatile material in technology. Applications extend from optical fibers, transparent structures, and biosensor structures to its critical role in microelectronics owing to its amazingly good interface with Si. The latter is the critical property that has enabled all of modern computing and communications. Consequently, much is known about its chemistry, and broad general knowledge has been established. One such accepted process is that SiO₂ dissolves in HF acid, leaving a hydrophobic H-terminated Si surface^{1,2} that is almost devoid of surface states. The dangling bonds are fully terminated,³ and this surface displays a high degree of inertness to further room temperature chemical reactivity.^{4,5} This hydrogen-terminated surface has become a “standard” for many surface science studies. It is of great interest to understand why other group IV compounds, including those with a Si atomic surface, (e.g., silicon carbide) behave differently.

Silicon carbide (SiC) is beginning to replace silicon for high-power, high-temperature applications and is being considered for high- and mid-voltage MOSFET devices. For electronic applications, the attraction of SiC stems from the ability to grow a thermal silicon dioxide passivating layer, similar to silicon, which suggests that the wet chemical cleaning methods (e.g., HF etching) that have been well developed for Si can be used for SiC. Another important attraction of silicon carbide comes from its stability and biocompatibility, important for biomedical uses, such as a material for implants (in bone tissues), stents in blood vessels, and substrate for biosensors. For these applications, understanding and controlling the surface termination of its surface is critical. In particular, performing HF etching is an important step that is common for these applications.

Stoichiometric SiO₂ can be thermally grown on both Si and SiC, and no major difference is expected with regard to bulk oxide etching by HF, as has been noted previously.⁶ HF etching of the bulk oxide proceeds by H₂O and SiF_x removal.⁷ The final surface termination is well understood in the case of silicon. As the last oxygen atoms are removed from the silicon surface, the topmost silicon layer is F terminated. As the reaction continues, the Si back bonds are polarized, making them susceptible to further attack by HF to remove the top fluorinated Si atom and leaving the second layer Si atom with H termination, as shown schematically in Figure 1a. The situation is quite different for SiC surfaces on both the Si-terminated and

[†] Vanderbilt University.

[‡] Present address: Cree Inc., Durham, NC.

[§] University of Texas at Dallas.

^{||} Accelrys, Inc.

[±] Korea Research Institute of Chemical Technology.

[#] Rutgers University.

- (1) Kern, W. *J. Electrochem. Soc.* **1990**, *137*, 1887–1892.
- (2) In *Handbook of Semiconductor Wafer Cleaning Technology-Science, Technology, and Applications*; Kern, W., Ed.; William Andrew Publishing/Noyes: East Windsor, New Jersey, 1993.
- (3) Yablonovitch, E.; Allara, D. L.; Chang, C. C.; Gmitter, T.; Bright, T. B. *Phys. Rev. Lett.* **1986**, *57*, 249–252.
- (4) Higashi, G. S.; Chabal, Y. J.; Trucks, G. W.; Raghavachari, K. *Appl. Phys. Lett.* **1990**, *56*, 656–658.
- (5) Graf, D.; Grundner, M.; Schulz, R.; Muhlhoff, L. *J. Appl. Phys.* **1990**, *68*, 5155–5161.

(6) Johnson, M. B.; Zvanut, M. E.; Richardson, O. *J. Electron. Mater.* **2000**, *29*, 368–371.

(7) Trucks, G. W.; Raghavachari, K.; Higashi, G. S.; Chabal, Y. *J. Phys. Rev. Lett.* **1990**, *65*, 504–507.

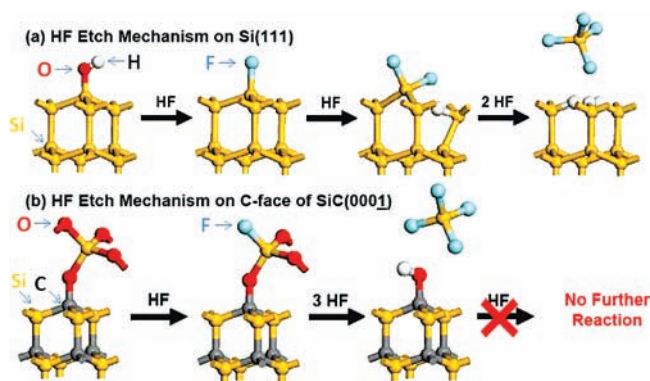


Figure 1. Schematic illustrations of mechanisms for (a) H passivation of Si(111) and (b) OH termination of (0001) the C-face SiC.

C-terminated surfaces, as schematically shown in Figure 1b and discussed below.

II. Background

Differences between Si/SiO₂ and SiC/SiO₂ interfaces have been noted in earlier works.^{8–13} Using ex-situ X-ray photoelectron spectroscopy (XPS), Sieber et al. reported that oxygen was present on the Si-face of 6H-SiC following HF treatment, although postcontamination in air could not be ruled out.¹¹ Seyller showed different low-energy electron diffraction (LEED) patterns between wet-cleaned and hydrogen-annealed 6H-SiC (0001) surfaces,¹⁰ suggesting that HF-etched SiC is not simply H terminated. Using vibrational spectroscopy after HF treatment of both (0001) Si- and (0001) C-terminated faces of 6H-SiC, Tsuchida et al. reported that surface-bound H (C–H_x, Si–H) was not detectable on either surface and instead presented evidence for the presence of some hydroxyl (OH) groups after HF treatment, possibly due to contamination in air.¹³ Surface wetting of SiC was also found to be different compared to Si surfaces.^{8,14,15} In particular, King et al. examined the wetting characteristics by immersion in a variety of acid/base solutions and found SiC surfaces to be mostly hydrophilic.⁸ More recently, evidence for oxygen on the surface was interpreted as due to the formation of a silicon oxycarbide (SiOC) alloy at the surface, associated with the initial thermal oxidation.¹⁶

All of these results indicate that SiC surfaces are chemically different than Si surfaces, but the origin of these differences is unclear. For instance, observation of oxygen and hydroxyl groups at the surface may simply be due to unstable H termination, as was found in the case of HF-etched germanium surfaces.^{17,18} In view of these observations, concerted efforts

are important to determine the chemistry of the etching processes and to understand the chemical properties of HF-etched SiC.

III. Methods

Silicon Carbide Sample Oxidation. The samples are research grade n-type 4H-SiC with 10 μm thick epilayers doped with nitrogen to about 10¹⁶ cm⁻³ purchased from Cree Inc. Two different crystal orientations are investigated, namely, the (0001) Si-face (8° off-axis) and the (0001) C-face (8° off-axis). All samples are initially oxidized at 1150 °C, in some cases using enriched ¹⁸O, and etching in HF/H₂O or DF/D₂O solutions. The use of the different isotopes allows an unambiguous determination of the source of the residual surface chemistry. Further details of the sample preparation are given in the Supporting Information.

Sample Preparation. Samples diced to 5 mm × 5 mm pieces were used for the NRA and contact angle measurements and quarters of 2 in. diameter wafers for IR experiments. Samples were degreased by ultrasonic cleaning sequentially in trichloroethylene (TCE), acetone, methanol, and deionized (DI) water and then immersed in dilute HF (5%). The samples were thermally oxidized in O₂ at 1150 °C for time periods necessary to grow approximately the same oxide thickness¹⁹ on all crystal faces (Si-face, 4 h; a-face and C-face, 1 h). Si(111) samples were also oxidized at 1000 °C as control samples. Oxide thicknesses were measured to be between 40 and 45 nm on all samples using spectroscopic ellipsometry. The samples were subsequently etched in solutions of a 1:1 D₂O: HF volume ratio (i.e., 25% HF) with deuterated water D₂O (99.9%, Cambridge Isotope Inc.) and HF (50% vol %, Fisher Chemical). Since the etch rate of SiO₂ in 5.0% HF is about 0.25 nm/s, etch times of 3–5 min were sufficient to remove the entire oxide layer on the samples. When solutions with other HF/D₂O volume ratios were used, the etching time was adjusted accordingly. After processing, the samples were dried by blowing nitrogen without any further rinsing.

Nuclear Reaction Analysis (NRA) and Rutherford Backscattering (RBS). NRA is one of the most reliable and quantitative experimental techniques for direct determination of elemental coverage on semiconductor surfaces.²⁰ In this work, the ¹⁸O(p,α)¹⁵N and ²H (³He,p) ⁴He nuclear reactions were employed for the detection and quantification of O and D species, respectively, on HF-etched SiC surfaces. A 2 MeV Van de Graaff electrostatic accelerator was used as the ion source for nuclear reaction analysis (NRA) and Rutherford backscattering spectroscopy (RBS). After etching, the samples were transferred to the analysis chamber (~10⁻⁷ Torr) within ~10 min. Annular solid-state detectors placed at ~180° were used for the detection of emitted nuclear reaction products and backscattered ions in the case of NRA and RBS, respectively. In addition, for NRA, a ~17 μm Al foil was placed in front of the detector to stop the backscattered primary ions. Standards were employed for absolute calibration of the NRA results.

X-ray Photoelectron Spectroscopy (XPS). Photoelectron spectra were measured with a Perkin-Elmer 5600 ESCA system, using an Al Kα monochromatic radiation of 1486.6 eV. Typically, the vacuum for measurement was 5 × 10⁻¹⁰ Torr. All XPS spectra were measured with a step of 0.125 eV using a pass energy of 58.7 eV. The data were collected at three different angles, 15°, 45°, and 75°, as defined by the position of the detector relative to the normal of the surface sample.

IR Absorption Experiments Using Attenuated Internal Reflection (GeATR). Infrared absorption spectroscopy was performed by bringing the etched surfaces in close contact (within 10–100

- (8) King, S. W.; Nemanich, R. J.; Davis, R. F. *J. Electrochem. Soc.* **1999**, *146*, 1910–1917.
 (9) Nakanishi, S.; Tokutaka, H.; Nishimori, K.; Kishida, S.; Ishihara, N. *Appl. Surf. Sci.* **1989**, *41–2*, 44–48.
 (10) Seyller, T. *J. Phys.: Condens. Matter* **2004**, *16*, S1755–S1782.
 (11) Sieber, N.; Seyller, T.; Graupner, R.; Ley, L.; Mikalo, R.; Hoffmann, P.; Batchelor, D. R.; Schmeisser, D. *Appl. Surf. Sci.* **2001**, *184*, 278–283.
 (12) Starke, U.; Bram, C.; Steiner, P. R.; Hartner, W.; Hammer, L.; Heinz, K.; Muller, K. *Appl. Surf. Sci.* **1995**, *89*, 175–185.
 (13) Tsuchida, H.; Kamata, I.; Izumi, K. *J. Appl. Phys.* **1999**, *85*, 3569–3575.
 (14) Catellani, A.; Cicero, G.; Galli, G. *J. Chem. Phys.* **2006**, *124*.
 (15) Teraji, T.; Hara, S. *Phys. Rev. B* **2004**, *70*.
 (16) Correa, S. A.; Radtke, C.; Soares, G. V.; Baumvol, I. J. R.; Krug, C.; Stedile, F. C. *Electrochem. Solid-State Lett.* **2008**, *11*, H258–H261.
 (17) Rivillon, S.; Chabal, Y. J.; Amy, F.; Kahn, A. *Appl. Phys. Lett.* **2005**, *87*.

- (18) Amy, S. R.; Chabal, Y. J. *Advanced Gate Stacks for High-Mobility Semiconductors*; Springer: Berlin, 2007; pp 73–113.
 (19) Song, Y.; Dhar, S.; Feldman, L. C.; Chung, G.; Williams, J. R. *J. Appl. Phys.* **2004**, *95*, 4953–4957.
 (20) In *Fundamentals of Surface and Thin Film Analysis*; Feldman, L. C., Mayer, J. W., Eds.; Elsevier: New York, 1986.

nm) with a Ge prism and performing single-reflection attenuated total internal reflection (ATR) spectroscopy (using a Harrick Scientific GATR). Absorption spectra were recorded with a Nicolet 6700 Fourier transform infrared spectrometer equipped with a liquid-nitrogen-cooled mercury cadmium telluride (MCT) detector using oxidized SiC as reference and averaging typically 5000 scans.

Contact Angle Measurements. Contact angle measurements were performed with a Ramé-Hart CA Goniometer. The sessile drop technique was used with a drop of 2 μL . The data shown are the average of at least three measurements taken in different locations of the samples.

Density Functional Theory (DFT). Density functional theory (DFT) calculations were carried using the DMol3 electronic structure package.²¹ The surface reaction sites were represented using fully periodic models based on 2×2 supercells of a 4-layer hydrogen-terminated slab of the HO/Si(111), HO/SiC(0001), and HO/SiC(000 $\bar{1}$) surfaces (with a 30 Å vacuum layer). Calculations were performed using the gradient-corrected PBE functional.²² A numerical atomic basis set of double- ζ quality augmented with additional polarization functions (DNP) with a real-space cutoff of 6.0 Å was employed in this work.²³ A Monkhorst-Pack k -point mesh with a spacing of 0.04 \AA^{-1} was used to sample the Brillouin zone. Minimum energy structures for the reactants, transition structures, and product species for the HF etch reaction were calculated at each of the surfaces. The nature of the calculated structures was verified by subsequent harmonic frequency calculations, which also yielded zero-point energy (ZPE) corrections. The top layer Si or C atomic charges reported here are Hirshfeld charges which are computed based on the difference between the molecular and the unrelaxed atomic charge densities.²⁴

IV. Results

The current effort is initially focused on characterizing the effect of HF etching on the final oxygen layer in contact with the underlying substrate for the Si- and C-faces of SiC and then on determining the chemical termination of the surface and its reactivity. To this end, a number of techniques with *elemental* and *chemical* sensitivity are combined with first-principles calculations. These include nuclear reaction analyses (NRA), X-ray photoelectron spectroscopy (XPS), and infrared (IR) absorption spectroscopy. In contrast to the hydrogen-terminated, hydrophobic Si surface, HF-etched SiC surfaces are found to be hydrophilic with a stable hydroxyl (OH) termination. This hydroxyl termination occurs on both faces of SiC and is due to the inability of HF to remove the last oxygen layer of the thermally grown silicon dioxide. Furthermore, the hydroxylated C-face of SiC is shown to be remarkably stable to the most aggressive chemical treatments. We employ gradient-corrected density functional theory (DFT) to rationalize these findings in terms of the reaction barriers and enthalpy associated with the various chemical processes. These results underscore the importance of kinetic control of surface chemistry with small changes in reaction barriers leading to qualitative differences in the resulting surface bonding.

a. Surface Wetting. An immediate visual indication as to the different behavior of Si and SiC under HF etching is the shape of the residual droplet of liquid at completion of the etching process. The measured contact angles (CA) for C- and Si-terminated SiC surfaces are $24^\circ \pm 1^\circ$ and $4^\circ \pm 1^\circ$, respectively, compared to 85° for Si after HF etching. These values are close

to the CA for SiO₂ surfaces ($CA \leq 4^\circ$), suggesting the presence of hydrophilic surface oxygen, in good agreement with previous observations on similar surfaces.⁸

b. Elemental Composition: NRA. The elemental *composition* of the etched surface is first established with nuclear reaction analysis sensitive to the presence of oxygen (mass 18 isotope, ¹⁸O) and deuterium (D). The main result of the ion-scattering analysis (Supporting Information) is that both HF (deuterium enriched)-etched SiC surfaces are left with approximately a full monolayer of original oxygen (i.e., from the grown isotopically enriched oxide) and the C face retains a large amount of hydrogen (deuterium from the etching solution). This observation unambiguously confirms that all of (and only) the last monolayer of oxygen from the SiO₂ remains on the surface bonded to the SiC substrate. This behavior is in sharp contrast to the HF(DF)-etched Si(111) surface, which is oxygen free and shows precisely one monolayer of H (D) coverage only.

c. Surface Chemical States: XPS. XPS measurements further identify and quantify the *chemical state* of species on the surface after etching. A survey scan shows that there is a barely detectable F signal (a small fraction of a monolayer) similar to that observed on silicon.⁵ The carbon core level (C1s) shows distinct components. On the C-terminated surface, the strongest peak is at 282.3 eV and assigned to C in bulk SiC. A weaker carbon feature at 283.7 eV is associated with surface carbon, as confirmed by angle-dependent experiments (Figure 2a). A similar core level position has been observed in other materials, such as Si₄C_{4-x}O₂ and Si₄C₄O₄, and assigned to carbon in a solid bound to oxygen.²⁵ For the C-face of the SiC surface, the only reasonable interpretation is the formation of a C–O bond on the surface carbon atoms, consistent with the NRA observation of a residual oxygen monolayer. The weakest component at 285 eV is associated with carbon contamination (e.g., hydrocarbons).²⁵ Assuming that the core level at 283.7 eV is associated with the last carbon layer, the concentration of this surface carbon (bound to oxygen) is estimated to be $8.5 \times 10^{14} \text{ cm}^{-2}$ ($\sim 70\%$ of a monolayer). The remnant of the surface is occupied by Si atoms, most likely resulting from steps. Indeed, angle-resolved XPS measurements of the Si 2p core level indicate the presence of *surface* Si atoms that are also bound to oxygen (Figure 2b insert). These atoms are characterized by a Si 2p core level at 101.1 eV (i.e., these atoms are also bound to oxygen atoms), and their concentration is estimated at $3.4 \times 10^{14} \text{ cm}^{-2}$. The presence of $\sim 30\%$ monolayer Si atom is consistent with the substrate miscut and atomic roughness of the surfaces. Together, *the concentration of C and Si makes up a monolayer*, in excellent agreement with the oxygen concentration of 1.0 ± 0.1 monolayer, measured from the O1s core level (Supporting Information).

On the Si-terminated surface (insert in Figure 2b), deconvolution of the Si 2p intensity yields three components at 100.5, 101.5, and 103.1 eV, as shown in Figure 2b. The weakest peak at 103.1 eV is typical of silicon in a high oxidation state (Si²⁺ and Si³⁺). This observation is consistent with both the higher oxygen concentration measured by ion scattering and the higher hydrophilicity of the Si-SiC surfaces as compared to the C-SiC surfaces. From angle-dependent measurements, we conclude that the component at 100.5 eV corresponds to bulk silicon in SiC and the component at 101.5 eV to surface silicon. The 101.5 eV peak indicates that each surface Si atom is *bound to one oxygen atom only*. Indeed, previous work has identified this core

(21) Delley, B. *J. Chem. Phys.* **2000**, *113*, 7756–7764.

(22) Perdew, J. P.; Burke, K.; Ernzerhof, M. *Phys. Rev. Lett.* **1996**, *77*, 3865–3868.

(23) Delley, B. *J. Chem. Phys.* **1990**, *92*, 508–517.

(24) Hirshfeld, F. L. *Theor. Chem. Acc.* **1977**, *44*, 129–138.

(25) Hornetz, B.; Michel, H. J.; Halbritter, J. *J. Mater. Res.* **1994**, *9*, 3088–3094.

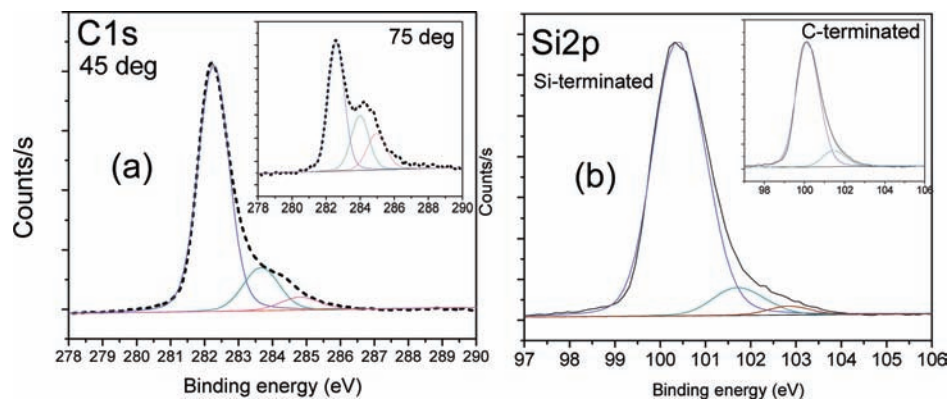


Figure 2. (a) X-ray photoelectron spectra of the carbon 1s core level on the C-face SiC measured at different incident angles, 45° and 75° (insert), yielding increasingly higher surface sensitivity. This measurement makes it possible to distinguish bulk from surface species. (b) X-ray photoelectron spectra of the silicon 2p core level on the Si-face SiC and C-face SiC (insert). A third component at ~103 eV (assigned to SiO₂) is required to obtain an acceptable fit for the Si-face SiC surface. Peak assignments and surface concentrations derived from XPS measurements performed at 45° are shown in Table S2 in the Supporting Information.

level shift with the presence of Si¹⁺, such as =Si–O–Si=, Si₄C_{4–x}O₂, and Si₄C₄O₄.²⁵ On this surface, there is also some surface carbon bound to oxygen (component at 284.0 eV in the C 1s core level spectrum). While these Si and surface C atoms form a monolayer, the amount of oxygen is substantially higher than a monolayer. Using an estimate similar to that done for the C-face SiC surfaces, the total amount of oxygen is estimated at 2.0 ± 0.1 monolayers (Supporting Information). This higher amount of oxygen agrees with the trend of the NRA results. It is also accounted for by the presence of SiO₂ formed during postoxidation of Si-rich regions, which further increases hydrophilicity, i.e., the amount of hydroxyls on the surface. An estimation of the oxygen layer thicknesses on top of the SiC bulk shows that this overlayer is in the range of 0.15–0.3 nm for both surfaces. These thicknesses are in the monolayer range on top of the SiC bulk (Supporting Information).

In summary, the XPS data show that for the C-face the surface carbon atoms are predominantly bound to oxygen and there is a substantial (~30%) component of surface Si also bound to oxygen. The Si-terminated surface gives clear evidence for single Si–O bonding with a weaker component of Si in higher oxygen bonding states and some indication of C–O bonding.

d. Surface Chemical Termination: Infrared Absorption Spectroscopy. Infrared absorption spectroscopy is well suited to determine the *local chemical structure* of the surface, particularly with respect to the bonding of H or D to the surface. Using an attenuated total reflection (ATR) configuration (Supporting Information), it is possible to measure and distinguish all hydrogen/deuterium configurations that could potentially be formed such as CH_x, SiH_x, C–OH, Si–OH, and their deuterated analogues at the monolayer level. For these experiments, the oxides on the Si- and C-faces of 4H-SiC and on (111) Si (for comparison) are etched using a 1:3 volume ratio of HF and D₂O. Similar HF treatment of oxidized Si(111) surfaces clearly show Si–H and Si–D vibrations (not shown).⁴ After obtaining the IR absorption spectra of the etched SiC surfaces, the samples are immersed in boiling sulfuric acid/hydrogen peroxide (piranha solution) and examined again, the assumption being that the latter treatment removes all hydrogen/deuterium by reoxidation.

The spectral results obtained on C-terminated SiC are shown in Figure 3a for HF:D₂O and Figure 3b for HF:H₂O treatments. Besides a strong multiphonon absorption at ~2150 cm⁻¹ (arising from changes in sensitivity to substrate upon oxide removal) there are clear absorption bands at 2450 and 3350 cm⁻¹ for the

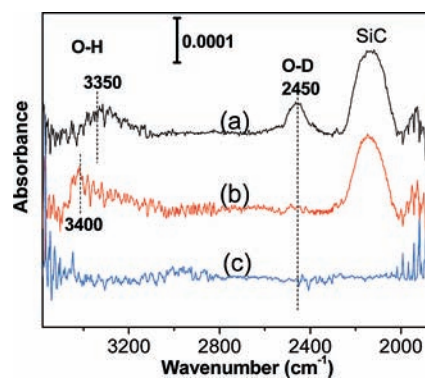


Figure 3. Infrared absorption spectra of the C-face 4H-SiC surfaces after etching of the oxide overlayer using (a) HF:D₂O and (b) HF:H₂O. Spectra a and b are referenced to the surface before etching. (c) Infrared absorption spectra of the C-face 4H-SiC etched with HF:D₂O subsequently treated 10 min in a piranha solution (c is referenced to the surface before treatment in the piranha solution). The piranha solution does not induce any change on the surface, that is, no exchange of the O–D to O–H.

HF:D₂O-treated surface and at ~3400 cm⁻¹ for the HF:H₂O-treated surface, assigned to O–D and O–H stretching modes, respectively. These frequencies (2450 and 3350 cm⁻¹) are substantially lower than those of typical silanols on Si (2650 and 3660 cm⁻¹) but are expected for C–OH structures (alcohol termination, as described below). For the HF-treated SiC surface, the blue shift (from 3350 to ~3400 cm⁻¹) of the O–H stretch is expected because a full monolayer is formed i.e. OH–OH dipole coupling. Using fully hydrogenated Si(100) and partially hydroxylated Si(100) surfaces as reference,²⁶ the coverage of OH is estimated to be 0.7 ± 0.2 monolayer (Supporting Information). Importantly, on both HF:D₂O- and HF:H₂O-treated surfaces, there is no evidence for the formation of C–H or Si–H termination.

Strong oxidizers invariably remove all H passivation of silicon surfaces via oxidation of silicon. Therefore, the *absence* of deuterium removal shown in Figure 3c is particularly surprising. Figure 3c reveals that the O–D-terminated surface is completely stable against further oxidation and H/D isotopic exchange when immersed in a hot sulfuric acid/hydrogen peroxide solution. While the stability of the O–D bond is not unexpected in a

(26) Chabal, Y. J.; Christman, S. B. *Phys. Rev. B* **1984**, *29*, 6974.

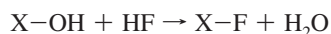
strong acid ($\text{pH} \ll 1$),^{27,28} the lack of oxidation by this strong oxidizer is clearly different from that observed on deuterium-terminated *silicon* surfaces. In acidic media, HF-etched C-SiC surfaces are terminated by hydroxyls and stable against the most aggressive chemical treatments because the underlying substrates cannot be oxidized.

The stability of the O–H functionality on the Si-SiC surface is different. While the topmost oxygen remains stable against HF etching and acid treatment, there is no evidence of deuterium at the surface. No O–D stretching modes are evident in the IR or in the NRA results, which is consistent with the deuterium undergoing release or exchange. It is well established that silanols are far more acidic than their corresponding carbinol analogues due to a large difference in electronegativity (Pauling, 1.9 and 2.6).²⁹ The more electropositive Si better stabilizes the resulting oxygen anion, leading to a lower deprotonation energy, which results in higher acidity and facile proton exchange.³⁰ The atomic charges calculated using density functional theory for the topmost SiC substrate atoms are -0.16 and 0.35 for C and Si, respectively.

V. Discussion and Modeling

As illustrated schematically in Figure 1b, the diverse experimental measurements described here provide a consistent picture revealing that the HF-treated SiO_2/SiC surface is characterized by a full monolayer of bonded oxygen arising from the original oxide with a substantial fraction of the oxygen further bonded to hydrogen in a hydroxyl termination. Therefore, both the carbon and the silicon surfaces of SiC have a markedly different surface termination than the pure hydrogen termination of silicon.

To gain insight into the dramatic differences in surface reactivity and final termination upon HF treatment, density functional theory was used to analyze the kinetics and thermodynamics of the HF etching reaction on Si and SiC surfaces. The reaction considered is



where X represents the underlying top layer substrate atom for each surface ($\text{X} = \text{Si}$ on Si(111), Si on SiC(0001), and C on SiC(000 $\bar{1}$)). The energy profiles for HF reaction at the HO/Si(111), HO/Si-SiC, and HO/C-SiC surfaces are presented in Figure 4 (denoted \bullet , \diamond , and \circ , respectively). The potential energy surface for the HF etching reaction has a central barrier, associated with the transition structure, separating the reactant and product channels which are characterized by molecule/surface reactant and product complexes. The critical point structures for these surfaces are similar to those shown for HO/Si(111) in Figure 4 (top), where the separated reactants, reactant-complex, transition state, product-complex, and separated products are denoted R, RC, TS, PC, and P, respectively. The reference system for assessing the relative reactivities of SiC substrates is the Si(111) surface. The HF + HO/Si(111) process is predicted to have a barrier of 0.67 eV with the final products 0.37 eV lower in energy than the reactants. These results are consistent with previous calculations finding the HF + HO/

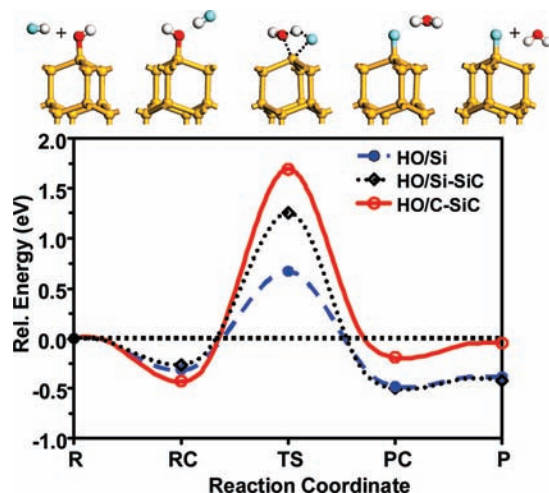


Figure 4. (Top) Structures optimized within density functional theory for each critical point involved in the removal of $-\text{OH}$ by HF to form SiF at the Si(111) surface. (Bottom) Reaction energy profiles for HF etching surface reaction pathways with the Si(111) and Si- and C-face SiC surfaces. [R, RC, TS, PC, and P indicate the reactants, reactant-complex, transition state, product-complex, and products, respectively.]

Si(111) \rightarrow F/Si(111) + H_2O reaction to be both thermodynamically and kinetically favorable.^{7,31}

The difference in reaction energetics between the Si and the SiC surfaces provides critical insight toward understanding the different HF etching surface products. As shown in Figure 4, the activation energies for removal of surface OH (replacement by F) at the Si- and C-face SiC surfaces are substantially higher (1.25 and 1.69 eV, respectively) than for the Si surface. While the overall reaction enthalpy for fluorination of OH-Si(SiC) and OH-Si(Si) is similar (0.42 eV exothermic), the C-face SiC is thermoneutral. Therefore, the HF etching reaction that is highly effective for Si surfaces is kinetically hindered at oxidized SiC surfaces that consequently remain hydroxyl terminated. The surface oxygen from the last oxide layer cannot be removed under the experimental conditions.

These calculations also yield the vibrational frequencies of the critical structures, such as the O–D and O–H stretch modes. Calculated vibrational frequencies are in excellent agreement with experimentally resolved IR absorption bands for O–H and O–D bonded to C on the SiC surface (theory (H/D), 3351/2440 cm^{-1} ; expt (H/D), 3350/2450 cm^{-1}). The key experimental observation, stability of the surface oxygen, is therefore well explained by the theoretical calculations.

These findings indicate that the presence of oxygen is primarily due to hydroxyl termination. This finding is in contrast to the interpretation of Correa et al.¹⁶ that attributed the presence of oxygen to the formation of an oxycarbide alloy at the surface. In fact, our DFT calculations show that the insertion of oxygen into the Si–C back-bond to form oxycarbide is energetically unfavorable, being endothermic by ~ 4 eV.

V. Conclusions and Outlook

In summary, a diverse set of analytical measurements have been applied along with first-principles calculations to obtain a consistent and detailed understanding of the effect of HF etching at SiO_2/SiC interfaces. In contrast to the well-known hydrophobic H-terminated surfaces derived from oxidized Si surfaces,

(27) Grunwald, E.; Eustace, D. In *Proton Transfer Reactions*; Caldin, E. Gold, V., Eds.; Chapman and Hall: London, 1975; pp 103–120.

(28) Grunwald, E. *J. Phys. Chem.* **1963**, *67*, 2211.

(29) West, R.; Baney, R. H. *J. Am. Chem. Soc.* **1959**, *81*, 6145–6148.

(30) Damrauer, R.; Simon, R.; Kremp, M. *J. Am. Chem. Soc.* **1991**, *113*, 4431–4435.

(31) Hoshino, T.; Nishioka, Y. *J. Chem. Phys.* **1999**, *111*, 2109–2114.

HF etching of oxidized SiC yields hydrophilic, hydroxyl-terminated surfaces.

The stability and hydrophilicity of the $-OH$ layer on the C-face of SiC have important implications for subsequent surface reactions. For instance, as shown in the Supporting Information, the hydroxyl termination of SiC surfaces makes it possible to graft self-assembled silane molecules onto HF-etched SiC surfaces with high packing densities. The higher stability of the OH-terminated C-SiC surfaces presents a higher barrier for the process, but typical C-SiC surfaces have a high enough step density and atomic roughness to present enough Si surface atoms for grafting (Supporting Information Figure 1S).

This finding has profound implications for the use of SiC for biomedical applications because its termination directly affects the interaction of such surfaces with proteins. For example, it is known that cell cultures preferentially adhere to substrates with high wettability.^{32,33} Therefore, the residual and stable hydroxyl termination on HF-treated C-SiC surfaces will have important consequences for applications requiring biocompatibility.³⁴ In contrast, the ability to graft hydrophobic SAMs on Si-SiC provides an alternative functionality for stents. The respective reactivities of Si-SiC and C-SiC are also important for microelectronic applications, such as the growth of high-k dielectrics on SiC substrates.

Finally, these results provide new insights into the complex problem of the structure of the SiC/SiO₂ interface as employed in power devices, namely, there is no evidence for a residual, nonetchable, nonstoichiometric oxide at the interface. Rather the residual surface, although far from perfect, can be understood in terms of chemical concepts of binding and reaction barriers.

Acknowledgment. The work at UT Dallas (including XPS, IR, and contact angle measurements) was supported by the National Science Foundation (CHE-0827634). Part of this work at Vanderbilt was supported by DARPA Contract N00014-02-1-0628, ONR Grant N000140110616, NSF Grant No. DMR-0218406, the U.S. Army Research Laboratory (W911NF-07-2-0046), and the U.S. Defense Advanced Research Projects Agency (W56HZV-06-C-0228). Support for S. Choi was provided by the IT Scholarship Program supervised by IITA (Institute for Information Technology Advancement) & MIC (Ministry of Information and Communications), Republic of Korea. The authors are indebted to Dr. Bridget R. Rogers (Vanderbilt University) for initial XPS analyses and Dr. John R. Williams (Auburn University) for insightful and useful discussions. Computational resources from Hewlett-Packard are also gratefully acknowledged.

Supporting Information Available: Experimental details of the nuclear reaction analysis (NRA) and results; XPS analysis, peak identification, coverage, and thickness estimation from the XPS analysis; summary and comparison of NRA and XPS; coverage estimation from IR absorption spectroscopy measurements; self-assembled monolayer adsorption on the C- and Si-face SiC after HF etching. This material is available free of charge via the Internet at <http://pubs.acs.org>.

JA9053465

-
- (32) Freshney, R. I. In *Culture of Animal Cells*; Sons, J. W., Ed.; John Wiley & Sons: Hoboken, NJ, 2005, pp 105–113.
- (33) Coletti, C.; Jaroszeski, M. J.; Pallaoro, A.; Hoff, A. M.; Iannotta, S.; Saddow, S. E. *Conf. Proc. IEEE Eng. Med. Biol. Soc.* **2007**, 2007, 5850–3.
- (34) Yakimova, R.; Petoral, R. M.; Yazdi, G. R.; Vahlberg, C.; Spetz, A. L.; Uvdal, K. *J. Phys. D: Appl. Phys.* **2007**, 40, 6435–6442.